Hadronic cross-section fluctuations

B. Blättel and G. Baym
Department of Physics, University of Illinois at Urbana-Champaign, 1110 West Green Street, Urbana, Illinois 61801

L. L. Frankfurt
NSCL, Michigan State University, East Lansing, Michigan 48824

H. Heiselberg
Niels Bohr Institute, Blegdamsvej 17, DK-2100 Copenhagen Ø, Denmark

M. Strikman
Department of Physics, Pennsylvania State University, University Park, Pennsylvania 16802
(Received 11 June 1992)

The physics of color transparency and color opacity is usefully incorporated into the dynamics of relativistic nuclear collisions through the concept of hadronic cross-section fluctuations. We show how such fluctuations can be consistently related to inelastic shadowing and diffractive dissociation. For the nucleon-nucleon system we find a rather large dispersion of the cross section around its mean value; for the π-nucleon system, experiment shows even larger fluctuations, as predicted in constituent quark models, due to the smaller number of degrees of freedom. We show how the third moment of the distribution is probed in proton-deuteron diffractive dissociation. We estimate the form of the cross-section distribution from available information; data up to $p_{\rm lab} = 300$ GeV indicate that the width of the distribution grows logarithmically with energy. The triple-Pomeron limit indicates that the fluctuations could grow by a factor of 2 from energies reached at CERN to energies reached at the BNL Relativistic Heavy Ion Collider, but more data are needed for a firmer prediction.

PACS number(s): 11.80.La, 12.40.Gg, 25.40.Ve, 25.75.+r

I. INTRODUCTION

Hadronic cross-section fluctuations are related to a wide range of phenomena observed in high-energy nuclear physics, including diffractive scattering, inelastic shadowing, as well as color transparency and color opacity effects. Our goal is to investigate the connection between these phenomena and to extract the distribution of cross sections, especially its shape, dispersion, and energy dependence, from experiment and extrapolation from theoretical models.

Hadrons have a substructure, and thus in collisions can interact in varying internal configurations [1, 2]. The concept of cross-section fluctuations arising from this substructure is applicable at high energies when their internal configurations can be regarded as frozen. More precisely, the condition is that the relevant configurations, the cross-section eigenstates of the interaction (T-matrix) [3, 4], remain coherent in the scattering. This requirement is satisfied when the time in which the incident hadron passes the target is smaller than the time-dilated lifetime of the particular cross-section eigenstate, i.e. [1, 5],

$$2R < 2p_{\rm lab}/(M^2 - m^2). \tag{1}$$

Here M is the mass of the inelastic cross-section eigenstate and m the ground-state mass of the hadron; R is a typical nuclear size, ~ 1 fm in pp collisions or ~ 5 fm for heavy targets. [For a discussion of the importance of (1) for separation of Fock components see Ref. [6].]

When the instantaneous configuration can be considered frozen, the scattering process should be calculated first for the particular configuration and then integrated over all configurations that satisfy (1), weighted by the probability of the configuration, as given by the wave function of the hadronic projectile. Therefore, at high energies the cross section σ of a hadron has to be replaced by a distribution $P(\sigma)$ around the mean value $\bar{\sigma}$. The moments of this distribution, which we study in the following, indicate a rather large dispersion around the mean.

For $\sigma \ll \bar{\sigma}$ the distribution is determined by the physics of color screening, that is, for hadrons in "small configurations," the interaction is suppressed because of the small spatial extent of the color fields in the hadron [7], an observation first made within the Low and Nussinov two-gluon-exchange model [7, 8]. This phenomenon can manifest itself in a variety of phenomena, including diffractive excitation of pions into two jets [2], color transparency [9, 10], nuclear shadowing [11], production of leading nucleons in nucleus-nucleus collisions [12–14], and production of hadrons at large x in hadron-nucleus collisions [6].

The other end of the distribution $P(\sigma)$ describes states in "large configurations," which experience a stronger interaction with the target ($\sigma > \bar{\sigma}$), a "color opacity" effect. Whether a configuration is "small" or "large" is not determined exclusively by the spatial distribution of the partons. The distribution of partons in momentum space, e.g., the number of wee partons in a hadron, affects its cross section as well. The concept of cross-section fluctuations takes into account all different configurations, regardless of their particular structure.

In earlier work [15, 16] we have shown how color transparency and opacity effects influence the dynamics of heavy-ion collisions, and can account for the large fluctuations experimentally observed in E_t distributions. Here we extend our earlier discussion by extracting in greater detail the distribution of cross sections. Such information, especially the broadening as a function of energy, is important for understanding fluctuations observed in the CERN experiments [energies reached at the BNL Alternating Gradient Synchrotron (AGS) are too low for the hadronic configurations to be frozen during the collision] and for making predictions for energies reached at the BNL Relativistic Heavy Ion Collider (RHIC) and possibly the CERN Large Hadron Collider (LHC). We further show how inclusion of cross-section fluctuations solves the long-standing problem of how to account for diffractive-dissociation processes in inelastic high-energy nuclear collisions. We further discuss how fluctuations in σ take into account the main features of the inelastic shadowing phenomenon.

The variance of the distribution of cross sections σ_{ij} for the successive scattering of hadron i with hadrons j and j' is defined by

$$\omega_\sigma = \frac{\langle \sigma_{ij}\sigma_{ij'}\rangle_I - \langle \sigma_{ij}\rangle_I \langle \sigma_{ij'}\rangle_I}{\langle \sigma_{ij}\rangle_I \langle \sigma_{ij'}\rangle_I}, \tag{2}$$

where $\langle\ \rangle_I$ denotes the average over all internal configurations. We will generally be concerned with nuclear targets, for which j and j' are nucleons. To the extent that one can neglect correlations between internal configurations of the target nucleons [the standard assumption in nonrelativistic description of nuclei, corresponding to neglecting the physics relevant to the European Muon Collaboration (EMC) effect], we may write

$$\omega_\sigma = \frac{\langle \sigma_i^2\rangle_I - \langle \sigma_i\rangle_I^2}{\langle \sigma_i\rangle_I^2}, \tag{3}$$

where σ_i is the cross section for scattering of projectile i on a nucleon. In the next two sections we show that the variance ω_σ is probed in hadron-deuteron scattering (Sec. II) as well as in diffractive dissociation (Sec. III). We also discuss there the energy dependence of ω_σ, compare the fluctuations for nucleon and pion projectiles, and study the next higher moment, i.e., $\langle\sigma^3\rangle_I$, which is accessible in hadron-deuteron diffractive dissociation (Sec. III B). Taking this experimental information into account, we estimate the shape of the cross-section distribution function (Sec. IV). In Sec. V we discuss ω_σ in the context of Reggeon exchanges to estimate its energy dependence in a region where no experimental information is currently available. We give a summary and an outlook on open problems in Sec. VI.

II. INELASTIC GLAUBER SHADOWING

A. Nucleon-nucleon cross-section fluctuations

The total cross section for the scattering of a nucleon on a deuteron is noticeably smaller than the sum of the individual nucleon-nucleon cross sections, an effect largely due to "eclipses" in which either the neutron or the proton lies in the shadow cast by the other. The effect of this shadowing has been estimated by Glauber [17]:

$$\sigma_{\rm D} = \sigma_n + \sigma_p - \sigma_n\sigma_p \left\langle \frac{1}{4\pi r^2}\right\rangle_{\rm D}. \tag{4}$$

The appearance of the product of the two cross sections immediately suggests that inclusion of cross-section fluctuations affects the shadowing contribution. This can be seen more clearly by starting with the elastic scattering amplitude for a projectile in configuration p hitting a deuteron, in which the neutron and proton are in internal configurations j and j', respectively:

$$\begin{aligned} F^p_{jj'}(\mathbf{q}) &= S(\tfrac{1}{2}\mathbf{q})f^{pj}_n(\mathbf{q}) + S(-\tfrac{1}{2}\mathbf{q})f^{pj'}_p(\mathbf{q}) + \frac{i}{2\pi}\int d^2q'\, S(\mathbf{q}'-\tfrac{1}{2}\mathbf{q})f^{pj'}_p(\mathbf{q}-\mathbf{q}')f^{pj}_n(\mathbf{q}') \\ &= 2S(\tfrac{1}{2}\mathbf{q})f^{pj}(\mathbf{q}) + \frac{i}{2\pi}\int d^2q'\, S(\mathbf{q}')f^{pj'}(\tfrac{1}{2}\mathbf{q}+\mathbf{q}')f^{pj}(\tfrac{1}{2}\mathbf{q}-\mathbf{q}'), \end{aligned} \tag{5}$$

a generalization of the expression of Franco and Glauber [18]. Here $f^{ij}(\mathbf{q})$ is the nucleon-nucleon scattering amplitude for nucleons in configurations i and j; $S(\mathbf{q})$ is the deuteron form factor, with $S(0) = 1$. Note that in the last step we have neglected differences between cross sections for different isospin channels, since they are not essential in the following. The N-N amplitude can be parametrized as

$$f_{ij}(\mathbf{k}-\mathbf{k}') = \frac{1}{4\pi}\sigma_{ij}(\alpha+i)e^{-(\mathbf{k}-\mathbf{k}')^2\beta/2} \tag{6}$$

so that $\alpha = {\rm Re} f_{ij}/{\rm Im} f_{ij}$.

After averaging over the internal configuration we obtain the total nucleon-deuteron cross section:

$$\begin{aligned}\sigma_{\rm D} &= \langle 4\pi {\rm Im} F(q=0)\rangle_I \\ &= 2\bar\sigma - \frac{1}{8\pi^2}\langle \sigma_{pj}\sigma_{pj'}\rangle_I (1-\alpha^2)\int d^2q' e^{-\beta q'^2} S(\mathbf{q}') \\ &= 2\bar\sigma - (1+\omega_\sigma)\Delta_{\rm el},\end{aligned} \tag{7}$$

where

$$\Delta_{\rm el} \equiv \frac{1}{8\pi^2}\bar\sigma^2(1-\alpha^2)\int d^2q' e^{-\beta q'^2} S(\mathbf{q}'); \tag{8}$$

$\Delta_{\rm el}$ is usually called the elastic shadowing contribution. From (7) we see that ω_σ introduces additional shadowing, also observed experimentally [19, 20], beyond the elastic contribution $\Delta_{\rm el}$. Such corrections, called inelastic shadowing contributions $\Delta_{\rm inel}$, have been interpreted theoretically as arising from the propagation of inelastic states between two scattering processes. The shadowing contributions decrease the total cross section:

$$\sigma_{\rm D} = 2\bar\sigma - \Delta_{\rm el} - \Delta_{\rm inel}. \tag{9}$$

Comparing (8) with (9) we find that

$$\omega_\sigma = \frac{\Delta_{\rm inel}}{\Delta_{\rm el}}, \tag{10}$$

which shows the connection, which we elaborate further in the next section, between cross-section fluctuations and inelastic Glauber shadowing [21].

Figure 1 shows the values for ω_σ obtained from $\Delta_{\rm el}$ and $\Delta_{\rm inel}$, as given by Murthy *et al.* [19] for n+D scattering, and Dakhno [22] for p+D scattering. All parametrizations lead to a good agreement with the experimental data, which exist up to $p_{\rm lab} = 340$ GeV, on $\sigma_{\rm tot}(n{\rm D})$ [19] and $\sigma_{\rm tot}(h{\rm D})$ [20] [although the lowest parametrization (D3) is somewhat worse]. For this reason we present in Fig. 1 only results of calculations in these parametrizations but not the raw data. The results for higher momenta are extrapolations; their validity is discussed in Sec. V.

The main features of ω_σ can be seen most easily in the calculation of Murthy *et al.* [19] of the inelastic shadowing contribution via

$$\Delta_{\rm inel} = 2\int S(t)\frac{d^2\sigma}{dM^2dt}dM^2dt, \tag{11}$$

an expression first derived by Gribov [1]. Here $d^2\sigma/dM^2dt$ is the cross section for producing a state X with mass M and four-momentum transfer squared t in the inclusive process $N+N \to N+X$.

If we evaluate (10) using (8) and (11), the result slightly depends on the properties of the deuteron via the form factor $S(t)$, a geometric effect due to an interplay of the magnitude of the nucleon cross section and the size of the deuteron. To eliminate this influence we consider the limit of a small cross section or equivalently a large deuteron size by assuming that $S(t)$ is of much shorter range than $d^2\sigma/dM^2dt$. We then obtain

$$\begin{aligned}\Delta_{\rm inel} &\approx 2\left(\int \frac{d^2\sigma}{dM^2dt}dM^2\right)_{t=0}\int S(t)dt \\ &= 2\left(\frac{d\sigma_{diff}}{dt}\right)_{t=0}\int S(t)dt,\end{aligned} \tag{12}$$

where the last equation follows since only the diffractive part of $d^2\sigma/dM^2dt$ should be included in the calculation [23]; the reason for this, and the corresponding range of the M^2 integration, will be discussed below. Using the short range assumption for $S(t)$ in $\Delta_{\rm el}$, (8), the variance of the cross-section fluctuations becomes

$$\omega_\sigma = \frac{16\pi}{\bar\sigma^2}\left(\frac{d\sigma_{\rm diff}}{dt}\right)_{t=0} = \left(\frac{d\sigma_{\rm diff}}{dt}\Big/\frac{d\sigma_{\rm el}}{dt}\right)_{t=0}. \tag{13}$$

After this overview, we now look at the calculation of ω_σ in more detail to see how the energy dependence follows from Eqs. (8), (10), and (11). The deuteron form factor used by Murthy *et al.* [19] is

$$S(t) = \alpha_1 e^{\beta_1 t} + \alpha_2 e^{\beta_2 t} \tag{14}$$

(with, e.g., $\alpha_1 = 0.55, \alpha_2 = 0.45, \beta_1 = 78.64$ GeV^{-2}, $\beta_2 = 18.68$ GeV^{-2}). The distribution of inelastic states was obtained from a fit to experimental data at high energies of the form

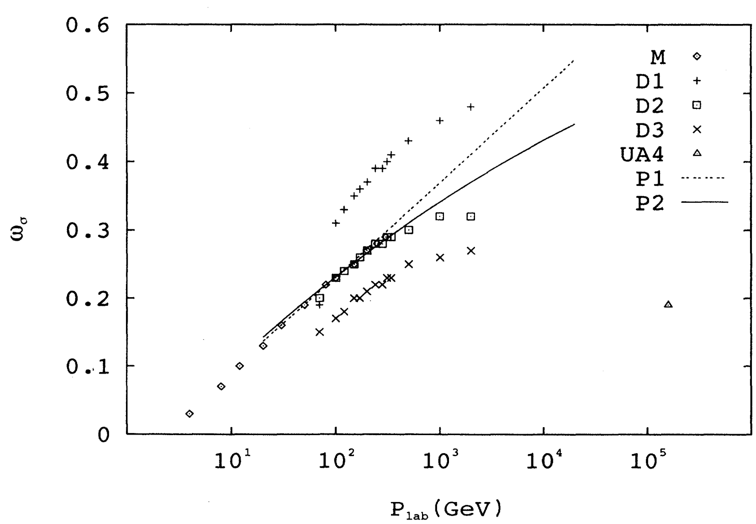

FIG. 1. Nucleon-nucleon cross-section fluctuations derived from Glauber shadowing via Eq. (10). The elastic and inelastic shadowing contributions are taken from Murthy *et al.* [19] (M) for pD scattering, and Dakhno [22] (D1-D3) for nd scattering. The point at 160 TeV is from p$\bar{\rm p}$ data of the UA4 collaboration [32]. The curves are extrapolations based on critical single Pomeron exchange (P1) given by Eq. (22), and the supercritical Pomeron (P2), Eq. (57).

$$\frac{d^2\sigma}{dM^2dt} = A(M^2)e^{B(M^2)t} \qquad (15)$$

where $A(M^2)$ and $B(M^2)$ are approximately energy independent.

In the analysis of Murthy *et al.*, the energy dependence of ω_σ is essentially due to $\Delta_{\rm inel}$, which contains t and M^2 integrations. As we will see, the energy dependence is due to the increasing contribution of higher mass states with growing energy. To see its trend, it is sufficient at high enough energies ($s \gg 6$ GeV^2) to evaluate the integral for $M^2 > M^2_{\rm min} = 6$ GeV^2. In this case the integrations simplify, since $A(M^2) = A_{\rm max}/M^2$ ($A_{\rm max} = 4.4$ mb/GeV^2) and $B(M^2) = B_{\rm max} = 6.6$ GeV^{-2} [19]. Performing the t integration in (11) with the limits

$$t_\mp = \frac{3}{2}m^2 + \frac{1}{2}M^2 - \frac{1}{2}s \pm \left[\left(\frac{1}{4} - \frac{m^2}{s}\right)\left((s - m^2 - M^2)^2 - 4m^2M^2\right)\right]^{1/2}, \qquad (16)$$

one obtains

$$\Delta_{\rm inel} = 2A_{\rm max}\int_{M^2_{\rm min}}^{M^2_{\rm max}} \frac{dM^2}{M^2} \sum_{i=1,2} \frac{\alpha_i}{\beta_i + B_{\rm max}} \left[e^{(\beta_i+B_{\rm max})t_-} - e^{(\beta_i+B_{\rm max})t_+}\right]. \qquad (17)$$

Because of the exponentials the significant contributions to the M^2 integral are only from $M^2 \ll s$, i.e., $M^2_{\rm max} = as$ ($a \ll 1$) where $t_- \approx 0$. The value of a follows from the exponential, which is dominated by the deuteron form factor ($\beta_1, \beta_2 > B_{\rm max}$). The form factor thus introduces a cutoff for the maximum mass of the inelastic intermediate state, which in fact guarantees the coherence or "frozenness" condition for the inelastic state. For $M^2 \gg m^2$, (1) implies that $2R \leq 2p_{\rm lab}/M^2$ and thus $M^2 \leq (2Rm)^{-1}s \approx 0.03s$, using $R \approx 3$ fm for the deuteron radius. It is this cutoff that defines the diffractive part $d\sigma_{\rm diff}/dt$ in terms of an integral of $d\sigma/dt\,dM^2$ over M^2. At first glance, this definition implies that ω_σ would depend on the size of the system (e.g., the deuteron) through a. However, since the energy-dependent part, which follows from the upper limit of the M^2-integration, is $\sim \ln as$, a only leads to a constant term in ω_σ and, therefore, becomes less relevant with increasing s. Thus, for $s \to \infty$, ω_σ becomes independent of the size of the specific system, and we obtain, from (17),

$$\Delta_{\rm inel} = b\,\ln(s/{\rm const}), \qquad (18)$$

with

$$b = 2A_{\rm max}\left(\frac{\alpha_1}{\beta_1 + B_{\rm max}} + \frac{\alpha_2}{\beta_2 + B_{\rm max}}\right). \qquad (19)$$

The value of the elastic shadowing term,

$$\Delta_{\rm el} = \frac{\bar\sigma^2}{8\pi^2}\left(\frac{\alpha_1}{\beta_1 + \beta} + \frac{\alpha_2}{\beta_2 + \beta}\right), \qquad (20)$$

follows from (8). In the limit $\beta_1, \beta_2 \gg \beta$ and $B_{\rm max}$, the result for ω_σ (10) no longer depends on the properties of the deuteron (i.e., $\alpha_1, \alpha_2, \beta_1, \beta_2$), and we obtain

$$\omega_\sigma = \frac{16\pi}{\bar\sigma^2}A_{\rm max}\ln(s/{\rm const.}). \qquad (21)$$

Note that although for $\beta_1, \beta_2 \to \infty$ the elastic and inelastic shadowing terms vanish, their ratio stays finite. Evaluating the integral (17) numerically (using $\bar\sigma = 39$ mb) we find

$$\omega_\sigma(s) \approx 0.06\,\ln(s/4\ {\rm GeV}^2). \qquad (22)$$

The results from Dakhno in Fig. 1 are the ratio of the inelastic to elastic shadowing corrections calculated in Ref. [22] using an analysis of the measured $d\sigma/dt\,dM^2$ [24–26] in terms of triple-Reggeon exchanges. The three different curves are from three different parameter sets obtained in Refs. [24–26] for the triple-Reggeon fits. These fits determine the high-energy limit of $d\sigma/dt\,dM^2$, for which $A(M^2)$ and $B(M^2)$ are energy independent. The variations in the three sets of results, a consequence of the inadequacy of the triple-Reggeon expansion, are a measure of the ambiguity of this extrapolation and hence the uncertainty in $\Delta_{\rm inel}$ and ω_σ. The errors are in agreement with Ref. [19], where uncertainties in the determination of $\Delta_{\rm inel}$ are estimated to be $\approx 40\%$.

It is important to realize, for future discussion, that the logarithmic rise of ω_σ is due to the $1/M^2$ dependence of $d^2\sigma/dM^2dt$ and the assumption of a constant NN cross section $\bar\sigma$. Although these assumptions are reasonable for the energy range considered ($p_{\rm lab} \approx 10 - 300$ GeV), one has to take the rise of $\bar\sigma$ into account in order to extrapolate ω_σ to higher momenta. Furthermore, since $\bar\sigma$ and $d\sigma/dtdM^2$ are related, this extrapolation has to be done in a consistent model for both quantities, as we discuss in Sec. V.

B. Meson-nucleon cross-section fluctuations

In Fig. 2 we show the cross-section fluctuations ω_σ obtained from the shadowing terms in πD scattering using (10). The values for $\Delta_{\rm el}$ and $\Delta_{\rm inel}$, taken from [22], are based on experimental results by Carroll *et al.* [20]. As one sees, the cross-section fluctuations for a pion projectile are significantly larger than for a proton projectile, a result expected in the framework of a constituent quark model, in which the pion has a smaller number of degrees of freedom that can fluctuate. A crude estimate of the influence of the number of valence quarks on the fluctuations can be obtained within a simple constituent quark

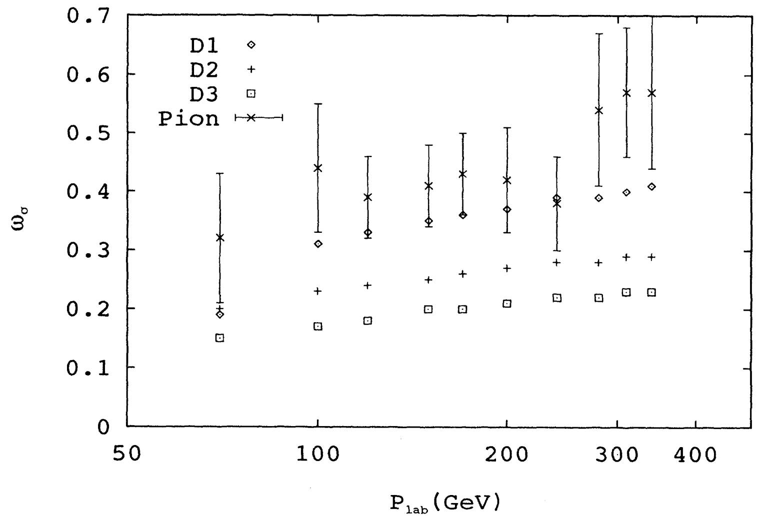

FIG. 2. Comparison of fluctuations ω for the nucleon-nucleon cross section and the pion-nucleon cross section. The nucleon-nucleon fluctuations are as in Fig. 1, where the differences between the three parametrizations (D1-D3) can be regarded as a measure of the error. The pion-nucleon fluctuations (pion) are calculated with the experimental $\Delta_{\rm inel}$ and the theoretical $\Delta_{\rm el}$ from Ref. [22] (dots with error bars).

model, as presented in [15, 13]. One assumes that the distribution of transverse sizes $r_\perp$ is given by $|\psi(r_\perp)|^2$. Quark counting rules suggest that this wave function has the asymptotic form $\sim r_\perp^{2(N_Q-2)}$ for small transverse radii (N_Q = number of valence quarks); we choose a Gaussian falloff for large $r_\perp$, so that

$$|\psi(r_\perp)|^2 = \exp(-r_\perp^2/r_c^2) r_\perp^{2(N_Q-2)}/r_c^{2(N_Q-1)}. \tag{23}$$

If the interaction between the colliding particles has a dipole-dipole form

$$\sigma_{pj} = \sigma(\mathbf{r}_{p\perp}, \mathbf{r}_{j\perp}) \simeq \bar{\sigma} \frac{r_{p\perp}^2 r_{j\perp}^2}{\langle r_\perp^2\rangle_p \langle r_\perp^2\rangle_j} \tag{24}$$

we obtain

$$\omega_\sigma^p = \frac{\langle \sigma_{pj}\sigma_{pj'}\rangle}{\langle\sigma_{pj}\rangle\langle\sigma_{pj'}\rangle} - 1 = \frac{\langle r_\perp^4\rangle_p}{\langle r_\perp^2\rangle_p^2} - 1 = \frac{1}{N_Q - 1}, \tag{25}$$

so that the fluctuations depend only on the properties of the projectile. For $N_Q = 3$ we obtain $\omega_\sigma^N = 0.5$ (as in [15]), whereas for $N_Q = 2$ the fluctuations double, i.e., $\omega_\sigma^\pi = 1$. The ratio $\omega_\sigma^\pi/\omega_\sigma^N = 2$ is roughly that found in Fig. 2.

The ratio $\omega_\sigma^\pi/\omega_\sigma^N$ can alternatively be estimated by calculating $d\sigma_{\rm diff}/dt$ and $d\sigma_{\rm el}/dt$ for NN and πN reactions using the triple-Reggeon limit, which is discussed in more detail in Sec. V. From the factorization principle one then obtains

$$\frac{\omega_\sigma^\pi}{\omega_\sigma^N} = \frac{\sigma^{NN}}{\sigma^{\pi N}} \approx \frac{40 \text{ mb}}{25 \text{ mb}} = 1.6, \tag{26}$$

which also supports the trend observed in Fig. 2. Note that Eq. (26) is not trivial; ω_σ as defined in Eq. (2) or (3) does not depend on the absolute value of σ. More detailed analysis of ω_σ for pion projectiles is presented in Ref. [27].

The same arguments as presented for the pion should apply to other mesons, e.g., the kaon. In this case factorization suggests that $\omega_\sigma^K/\omega_\sigma^N = \sigma^{NN}/\sigma^{KN} \approx 1.8$, a result that could be tested by further data on shadowing and diffraction of K-induced reactions.

The larger fluctuations of the pion-nucleon cross section should lead to an increase of the fluctuations in the number of inelastic collisions in high energy π-nucleus collisions compared to the nucleon-nucleus case. These fluctuations should be reflected in observations of multiplicity and transverse energy fluctuations, as discussed for proton-nucleus collisions in [15], and could be an interesting test for the phenomenon of color opacity [28]. The increased fluctuations of the pion-nucleon cross section suggests that color transparency should be greater for π-induced processes compared to proton-induced reactions. An experimental comparison of these two processes would be another important test of our understanding of cross-section fluctuations.

III. DIFFRACTIVE SCATTERING

A. Probing $\langle\sigma^2\rangle$ in $p+p$ scattering

In the collision of a hadron with a hadronic target at high energy a significant part of the total cross section is due to the production of inelastic states with the same quantum numbers as the incident particle, e.g., $p+p \to p+X$. This phenomenon of diffractive scattering [3, 4], which arises from the fact that the projectile is a composite object and its absorption by the target depends on its internal coordinates, contains information about the internal structure of hadrons; this can be seen explicitly by introducing cross-section eigenstates, as first proposed by Good and Walker [4]. We expand the hadronic state $|\Psi\rangle$,

$$|\Psi\rangle = \sum_k c_k|\psi_k\rangle, \tag{27}$$

in eigenstates $|\psi_k\rangle$ of the scattering amplitude $T = 4\pi F$, which we assume to be purely imaginary:

$$\text{Im}T|\psi_k\rangle = t_k|\psi_k\rangle; \tag{28}$$

the c_k are normalized by $\sum_k |c_k|^2 = 1$. The elastic scattering cross section is given by

$$\frac{d\sigma_{\rm el}}{dt} = \frac{1}{16\pi}|\langle\Psi|{\rm Im}T|\Psi\rangle|^2 = \frac{1}{16\pi}\left(\sum_k |c_k|^2 t_k\right)^2$$
$$= \frac{1}{16\pi}\langle {\rm Im}T\rangle^2. \tag{29}$$

Diffractive scattering occurs when the final state has the same quantum numbers as the nucleon, i.e., whenever it overlaps any $|\psi_k\rangle$; thus, subtracting the elastic contribution we can write

$$\left(\frac{d\sigma_{\rm diff}}{dt}\right)^{pp} = \frac{1}{16\pi}\sum_k |\langle\psi_k|{\rm Im}T|\Psi\rangle|^2 - \frac{d\sigma_{\rm el}}{dt}$$
$$= \frac{1}{16\pi}\left\{\sum_k |c_k|^2 t_k^2 - \left(\sum_k |c_k|^2 t_k\right)^2\right\}$$
$$= \frac{1}{16\pi}\left(\langle {\rm Im}T^2\rangle - \langle {\rm Im}T\rangle^2\right). \tag{30}$$

From the optical theorem (${\rm Im}T|_{t=0} = \sigma$) we obtain

$$\left(\frac{d\sigma_{\rm diff}}{dt}\right)^{pp}_{t=0} = \frac{1}{16\pi}\left(\langle\sigma^2\rangle - \langle\sigma\rangle^2\right) \tag{31}$$

so that (13) again follows for the variance ω_σ. This result was first derived by Miettinen and Pumplin [29], and interpreted in terms of color fluctuations [30]. However, one should note that $(d\sigma_{\rm diff}/dt)^{pp}$ in (31) is slightly different from the expression in (13), since the coherence condition for the pD system is different from that in the pp case. This effects the upper limit for the mass integration of $d\sigma/dt\,dM^2$ leading to $(d\sigma_{\rm diff}/dt)$. For the pp case, the frozenness condition is $M^2 \leq (2R_N m)^{-1}s \approx 0.1s$ (where R_N, the nucleon radius, is ≈ 1 fm), so that $M^2_{\rm max} = as$ with $a \approx 0.1$, compared to $a \approx 0.03$ for the pD system. However, as already mentioned, the different value only changes a constant contribution to ω_σ, which becomes irrelevant at high energies. Taking these small differences into account, the expression for ω_σ that follows from (31) is consistent with (10).

Miettinen and Pumplin [29] show M^2-integrated data from the CERN Intersecting Storage Rings (ISR) [31] for $p_{\rm lab} = 290 - 780$ GeV/c. Unfortunately the data are not good enough to allow one to infer $(d\sigma_{\rm diff}/dt)_{t=0}$ for each energy individually. An average over the whole energy interval gives $(d\sigma_{\rm diff}/dt)_{t=0} \approx 22$ mb/GeV^2. However, given the uncertainties in the cutoff for the mass integration, the true value could change by as much as 30% [31]. With an average cross section $\bar\sigma = 41$ mb for the energy interval considered, we obtain $\omega_\sigma = 0.26$ as a lower bound in this regime, which agrees with Fig. 1.

At the CERN Super Proton Synchrotron (SPS) collider the cross section for $\bar p + p \to \bar p + X$ has been measured by the UA4 Collaboration [32] at $\sqrt{s} = 546$ GeV, which corresponds to $p_{\rm lab} \approx 160$ TeV. With $\sigma_{\rm tot} = 60.5$ mb and $(d\sigma_{\rm diff}/dt)_{t=0} \approx 35$ mb/GeV^2, one obtains $\omega_\sigma \approx 0.19$, assuming that the differences between pp and $\bar pp$ scattering can be neglected at this energy. This small value of ω_σ, also shown in Fig. 1, suggests an interesting transition in the physics that causes a rising ω_σ to begin to decrease with energy (see further discussion in Sec. V) [33].

Kopeliovich and Lapidus [34] also made the connection between the distribution of cross-section eigenstates and the inelastic intermediate states used in the multiple scattering model for the calculation of inelastic Glauber shadowing, using the fact that in the "frozen" regime (1) the cross-section eigenstates do not mix during their interaction with the deuteron. One may see this connection as follows. Using the optical theorem, the second term ($\equiv \Delta F^p_{jj'}(t)$) in (5) implies the pD shadowing term

$$\Delta_{\rm tot} = 4\pi\sum_{p,j,j'} |c_p|^2|c_j|^2|c_{j'}|^2({\rm Im}\Delta F^p_{jj'})_{t=0}$$
$$= \left(\sum_p |c_p|^2 t_p^2\right)_{t=0}\frac{1}{8\pi^2}\int d^2q S(q)$$
$$= \frac{1}{8\pi^2}\langle\sigma^2\rangle\int d^2q S(q). \tag{32}$$

As in Eq. (12) we have assumed a short-range form factor $S(q)$ and made the identification

$$t_p = 4\pi\sum_j |c_j|^2 f^{pj}. \tag{33}$$

To obtain the elastic shadowing term one takes into account only elastic intermediate states, which is equivalent to averaging the scattering amplitudes in (5) separately, i.e.,

$$\Delta_{\rm el} = \frac{1}{8\pi^2}\int d^2q S(q)\sum_{j,j'}|c_j|^2|c_{j'}|^2\left(4\pi\sum_p |c_p|^2 f^{pj}\right)\left(4\pi\sum_p |c_p|^2 f^{pj'}\right)$$
$$= \frac{1}{8\pi^2}\langle\sigma\rangle^2\int d^2q S(q). \tag{34}$$

The inelastic contribution is therefore given by

$$\Delta_{\rm inel} = \Delta_{\rm tot} - \Delta_{\rm el} = \frac{1}{8\pi^2}(\langle\sigma^2\rangle - \langle\sigma\rangle^2)\int d^2q S(q). \tag{35}$$

We again see that the calculation of ω_σ from Glauber shadowing via (10) is consistent with its definition using cross-section eigenstates.

B. Probing $\langle\sigma^3\rangle$ in p+D scattering

Diffractive scattering on the deuteron involves both diffraction and shadowing, both of which exhibit a linear and quadratic σ dependence; this process thus probes the third moment $\langle\sigma^3\rangle$ of the cross-section distribution. The cross section for p+D$\rightarrow X + D$ can be calculated analogously to Eq. (30):

$$\left(\frac{d\sigma_{\rm diff}}{dt}\right)^{pD} = \frac{1}{16\pi}\left\{\sum_k |c_k|^2 T_k^2 - \left(\sum_k |c_k|^2 T_k\right)^2\right\}. \qquad (36)$$

In this case T_k is the elastic scattering amplitude for a proton cross-section eigenstate $|\psi_k\rangle$ [defined via (27)] scattering on a deuteron (k + D $\rightarrow k$ + D), and is given in terms of the amplitude in Eq. (5), i.e.,

$$T_k = 4\pi \sum_{j,j'} |c_j|^2 |c_{j'}|^2 F^k_{jj'}. \qquad (37)$$

Using (5), and $t \equiv q^2$, we obtain

$$\left(\frac{d\sigma_{\rm diff}}{dt}\right)^{pD} = \frac{1}{4\pi}\left(\langle({\rm Im}T)^2\rangle - \langle {\rm Im}T\rangle^2\right) \times\left(S^2(q^2/2) - \frac{1}{8\pi^2}\frac{\langle({\rm Im}T)^3\rangle - \langle{\rm Im}T\rangle\langle({\rm Im}T)^2\rangle}{\langle({\rm Im}T)^2\rangle - \langle{\rm Im}T\rangle^2} S(q^2/4)\int d^2p_\perp S(q_\parallel^2/4 + p_\perp^2)\right), \qquad (38)$$

where ImT is the NN scattering amplitude; we have neglected terms $\sim ({\rm Im}T)^4$, since they are of order $(\Delta_{\rm tot}/\sigma_{\rm tot})^2$. Furthermore, we have assumed that the deuteron form factor $S(t)$ is sharply peaked at $t = 0$, so that the scattering amplitudes can be pulled out of the integral. Using (30), we calculate the ratio of $p + p$ to p+D diffractive cross sections for $t \rightarrow 0$ (using ${\rm Im}T|_{t=0} = \sigma$):

$$\left(\frac{d\sigma_{\rm diff}}{dt}\right)^{pp}_{t=0}\Bigg/\left(\frac{d\sigma_{\rm diff}}{dt}\right)^{pD}_{t=0} = \left(4S^2(0) - \frac{1}{2\pi^2}\frac{\langle\sigma^3\rangle - \langle\sigma\rangle\langle\sigma^2\rangle}{\langle\sigma^2\rangle - \langle\sigma\rangle^2} S(0)\int d^2p_\perp S(p_\perp^2)\right)^{-1}. \qquad (39)$$

In order to compare this expression with calculations explicitly including intermediate inelastic states, we assume that, for $t \rightarrow 0$ at large s,

$$\left(\frac{d\sigma_{\rm diff}}{dt}\right)^{pp}_{t=0}\Bigg/\left(\frac{d\sigma_{\rm diff}}{dt}\right)^{pD}_{t=0} \approx \left(\frac{d\sigma}{dt\,dx}\right)^{pp}_{t=0}\Bigg/\left(\frac{d\sigma}{dt\,dx}\right)^{pD}_{t=0}, \qquad (40)$$

where x is the Feynman variable; for $M^2 \gg m^2$, one has $1-x = M^2/s$, so that $x \rightarrow 1$ for large s. Equation (40) is reasonable, since the ratio on the right side is to a good approximation independent of x, due to the fact that the inelastic cross section factorizes in the same way as the elastic one [35, 36], i.e.,

$$\left(\frac{d\sigma}{dt\,dM^2}\right)^{pD} = \left(\frac{d\sigma}{dt\,dM^2}\right)^{pp} F_{\rm D}(t), \qquad (41)$$

where $F_{\rm D}(t)$ is independent of M.

To determine $\langle\sigma^3\rangle$, we compare (39) [using (40)] to the corresponding expression resulting from explicit inclusion of inelastic intermediate states. The easiest way to include such effects, indicated diagrammatically in Fig. 3, results in the scattering amplitude

$$F_X(\mathbf{q}) = 2S(\tfrac{1}{2}\mathbf{q})f_X(\mathbf{q}) + \frac{i}{2\pi}\int d^2q' S(\mathbf{q}')f_X(\tfrac{1}{2}\mathbf{q}+\mathbf{q}') \times[f_{\rm el}(\tfrac{1}{2}\mathbf{q}-\mathbf{q}') + f_{X{\rm el}}(\tfrac{1}{2}\mathbf{q}-\mathbf{q}')], \qquad (42)$$

which is a generalization of (5) for the case of particle production and the propagation of inelastic intermediate states [38]. Here f_X is the amplitude for the production of the diffractive state X, while $f_{\rm el}$ and $f_{X{\rm el}}$ are the elastic NN and XN scattering amplitudes. Assuming that $f_{\rm el}$ has the same q dependence as $f_{X{\rm el}}$, one can write

$$F_X(\mathbf{q}) = 2S(\tfrac{1}{2}\mathbf{q})f_X(\mathbf{q}) + \frac{i}{2\pi}\delta\int d^2q' S(\mathbf{q}')f_X(\tfrac{1}{2}\mathbf{q}+\mathbf{q}')f_{\rm el}(\tfrac{1}{2}\mathbf{q}-\mathbf{q}'), \qquad (43)$$

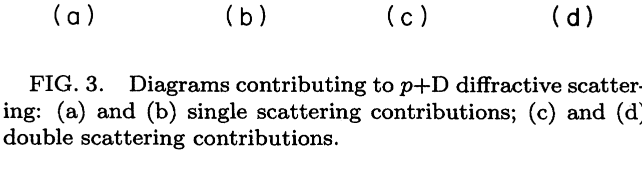

FIG. 3. Diagrams contributing to p+D diffractive scattering: (a) and (b) single scattering contributions; (c) and (d) double scattering contributions.

where we have introduced the rescattering parameter $\delta = 1 + \sigma_{XN}/\sigma_{NN}$.

Pion exchange contributes to pp diffractive scattering, but does not occur in pD scattering, since the deuteron has zero isospin. However, for small M^2/s, pion-exchange contributions can be neglected, and one finds

$$\left(\frac{(d\sigma/dt\,dx)^{pp}}{(d\sigma/dt\,dx)^{pd}}\right)_{x\to 1} = \frac{|f_X(t)|^2}{\left|2S(t/4)f_X(t) + \frac{1}{2}i\delta f_{\rm el}(t/4)f_X(t/4)\int dt' S(t')\right|^2}. \tag{44}$$

If we neglect terms $\sim f^4$ in the cross section, a comparison of (44) to (39) relates $\langle\sigma^3\rangle$ to the rescattering parameter via

$$\kappa_\sigma \equiv \frac{\langle\sigma^3\rangle - \langle\sigma\rangle\langle\sigma^2\rangle}{\langle\sigma\rangle^3} = \omega_\sigma\,\delta. \tag{45}$$

The value for $\delta = 1.7 \pm 0.25$ has been extracted from experimental data [39, 40] for $p_{\rm lab} = 154$ GeV and 372 GeV. A more complete analysis of the effects of inelastic intermediate states by Zamolodchikov *et al.* yields $\delta = \delta^{(Z)} - \lambda^{(Z)} = 1.98 \pm 0.16$, where $\delta^{(Z)}$ and $\lambda^{(Z)}$ are the variables defined in Ref. [37] without the superscript.

IV. THE FORM OF THE CROSS-SECTION DISTRIBUTION FUNCTION

We turn now to determining an analytic form for the cross-section distribution function. First we discuss how the form of $P(\sigma)$ at small σ is determined by quark counting rules and the dipolar form of the cross section. As discussed in Sec. II B, the cross section for a small-size configuration with radius $r_\perp$ is $\sigma \sim r_\perp^2$. The distribution of sizes follows from quark-counting rules, which imply that $|\Psi(r_\perp^2)|^2 \sim r_\perp^{2(N_q-2)}$ for small $r_\perp$. Therefore $\langle\sigma\rangle \sim \langle r_\perp^2\rangle \sim \int d^2r_\perp\, r_\perp^2 (r_\perp^2)^{N_q-2} \sim \int d\sigma\, \sigma P(\sigma)$, indicating that

$$P(\sigma) \sim \sigma^{N_q-2} \quad \text{for } \sigma \ll \bar\sigma. \tag{46}$$

Thus we expect, for small σ, $P(\sigma) \sim \sigma$ for a baryon ($N_q = 3$) and $P(\sigma)$ is constant for a meson ($N_q = 2$). The latter result implies that the distribution $P(\sigma)$ for a pion does not necessarily vanish for $\sigma \to 0$, another indication that color transparency effects for processes involving a pion are expected to be more pronounced than in nucleon-induced reactions. This effect is in addition to the larger fluctuations in the πN cross section, which should also enhance the transparency.

In the following, we discuss the form of $P(\sigma)$ for baryons, for which we have the most experimental information. As a first estimate we consider a Gaussian distribution modified to give the correct asymptotic behavior for $\sigma \to 0$; we write, in general,

$$P(\sigma) = N(a,n)\frac{\sigma/\sigma_0}{\sigma/\sigma_0 + a} e^{-(\sigma-\sigma_0)^n/(\Omega\sigma_0)^n}; \tag{47}$$

with $n = 2$ for a Gaussian. A numerical fit to a characteristic value $\omega_\sigma = 0.25$ (with $a = 1.0$) leads to $\kappa_\sigma = 2.26\omega_\sigma$, which is larger than the value obtained in the last section. Variation of a does not have a strong effect on $\kappa_\sigma/\omega_\sigma$; it is thus necessary to increase n, i.e., to introduce a much stronger falloff for $P(\sigma)$ at large cross sections. For $n = 6$, $a = 1.0$ one obtains $\kappa_\sigma/\omega_\sigma = 2.04$, whereas $n = 10$, $a = 1.0$ leads to $\kappa_\sigma/\omega_\sigma = 1.99$, both values within the experimental range. For $n = 6$, $a = 0.1$ (values which would, however, imply that the asymptotic behavior (46) would become relevant only at very small σ), the extracted $\kappa_\sigma/\omega_\sigma$ decreases only slightly to 2.00. The distributions for $n = 10$, $a = 1.0$ as well as $n = 6$, $a = 0.1$ are shown in Fig. 4 and compared to the

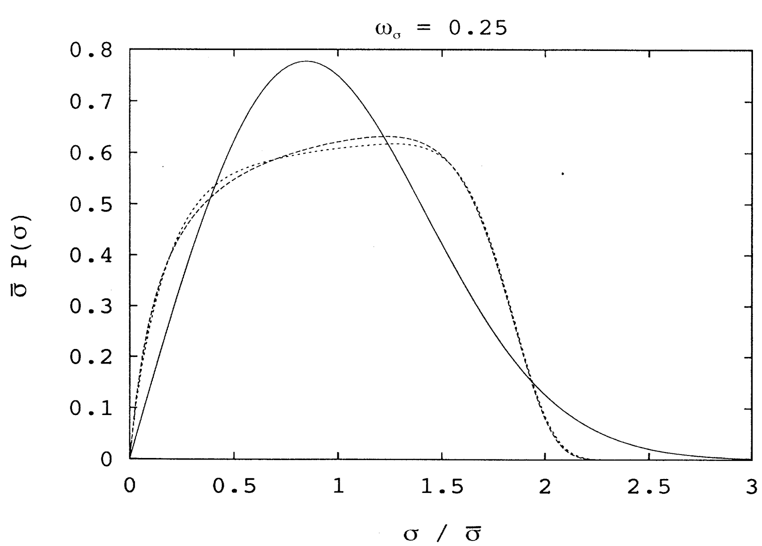

FIG. 4. Cross-section distribution functions $P(\sigma)$ [Eq. (47)] multiplied by $\bar\sigma$ versus $\sigma/\bar\sigma$, all with $\omega_\sigma = 0.25$. Solid line: $n = 2$, $\Omega = 1.5$, $a = 1.0$, $\sigma_0/\bar\sigma = 0.625$, $\bar\sigma N = 1.43$, $\kappa_\sigma/\omega_\sigma = 2.26$; dashed line: $n = 10$, $\Omega = 11.0$, $a = 1.0$, $\sigma_0/\bar\sigma = 0.155$, $\bar\sigma N = 0.72$, $\kappa_\sigma/\omega_\sigma = 1.99$; short dashed line: $n = 6$, $\Omega = 1.10$, $a = 0.1$, $\sigma_0/\bar\sigma = 0.893$, $\bar\sigma N = 0.66$, $\kappa_\sigma/\omega_\sigma = 2.00$.

modified Gaussian distribution.

To summarize, the rather small value $\kappa_\sigma/\omega_\sigma \approx 2$ found experimentally suggests a much more rapid falloff of $P(\sigma)$ for large cross sections, i.e., for $\sigma \gtrsim 1.7\bar{\sigma}$, than for a Gaussian. In comparison, the distribution obtained by Miettinen and Pumplin [29] has significant contributions at larger σ; it also does not have the expected behavior as $\sigma \to 0$. Our results imply that fluctuations with $\sigma > \sigma_{NN} + \sigma_{\pi N}$ are strongly suppressed. Further studies of κ_σ, especially its energy dependence, are capable of giving interesting information about cross-section fluctuations, especially for $\sigma > \bar{\sigma}$. In addition to p+D diffractive scattering, $p+{}^4$He diffraction, as well as shadowing in the total cross section for light nuclei (^{3}He, ^{4}He), may also provide such information.

V. THEORETICAL MODELS AND EXTRAPOLATION TO HIGH ENERGIES

Figure 1 shows that ω_σ increases with energy at least up to lab momenta of several hundred GeV. Unfortunately there is a gap in experimental information at higher energies, particularly in the range $p_{\rm lab} \approx 20$ TeV, the relevant regime for RHIC. At $p_{\rm lab} \approx 160$ TeV the one data point from the UA4 collaboration suggests a transition to a decreasing ω_σ. (But see Ref. [33].) More experimental data are needed to clarify the high energy trend of ω_σ.

As we now discuss, a first understanding of the initial rise of ω_σ with energy follows from the Reggeon exchange model. Provided that this physics dominates up to RHIC energies, this picture enables us to estimate roughly the fluctuations to be expected in future heavy-ion experiments. A more complete theoretical discussion of the physical processes underlying the energy dependence of ω_σ is an important problem to pursue in the future.

The Reggeon t-channel exchange model, which we use to study the high energy behavior of $\bar{\sigma}$ and $d\sigma/dt\,dM^2$, reproduces successfully many features of high-energy cross sections [41, 42]. Relating high energy (s-channel) scattering at small momentum transfer $\sqrt{t}$ to low energy (t-channel) annihilation processes using crossing symmetry, one finds that high energy reactions can be described by the exchange of Reggeons with trajectories, $\alpha_i(t)$, where i indicates the type of Reggeon that is exchanged. As indicated in Fig. 5(a), the total cross section for the reaction of two hadrons a and b is calculated by summing over the imaginary parts of the one-Reggeon exchange amplitudes at $t = 0$:

$$\sigma^{ab} = \sum_i \beta_i^{ab}(t=0)\left(\frac{s}{s_0}\right)^{\alpha_i(t=0)-1}. \tag{48}$$

We see that the exchanged Reggeon with squared momentum transfer t contributes with a factor $\sim \beta_i(t)(s/s_0)^{\alpha_i(t)}$ to the amplitude, where $\beta_i(t)$ is the residue and s_0 the appropriate scaling factor. In the single Reggeon-exchange model, unitarity requires $\alpha(t=0) \leq 1$ in the limit $s \to \infty$. Thus in the high energy limit only the Reggeon with $\alpha(t=0)=1$, the Pomeron, contributes, leading to a constant cross section

$$\sigma(s \to \infty) = \beta_P^{ab}(t=0). \tag{49}$$

In addition to describing total and elastic scattering cross sections the Reggeon-exchange model has been successfully applied to diffractive scattering processes (for a review see [36, 43]). The basic assumption is that $d\sigma/dt\,dM^2$ can be described for $M^2 > 5-7$ GeV^2 by replacing the coupling to the intermediate excited state by a triple Reggeon-vertex, as illustrated in Fig. 5(b), in which case (see, e.g., [36])

$$\frac{d\sigma}{dt\,dM^2} = \sum_{ijm} \beta_i(t)\beta_j(t)\beta_m(0)\frac{g_{ijm}}{16\pi^2}\left(\frac{s}{s_0}\right)^{\alpha_i(t)+\alpha_j(t)-2}\left(\frac{M^2}{s_0}\right)^{\alpha_m(0)-\alpha_i(t)-\alpha_j(t)}. \tag{50}$$

The argument 0 in one of the β functions follows directly from Fig. 5b. For $t=0$, the relevant part of $d\sigma/dt\,dM^2$ for the calculation of ω_σ and $s \to \infty$, only the contribution from the triple-Pomeron exchange survives and we obtain

$$\frac{d\sigma}{dt\,dM^2}(t=0, s\to\infty) = g_{PPP}\frac{\beta_P(0)^3}{16\pi^2}\frac{s_0}{M^2\alpha(0)}, \tag{51}$$

which, since $\alpha(0) \approx 1$, shows the $1/M^2$ behavior used in the parametrization of Murthy *et al.* [19]. One should note that in this limit only the diffractive part, i.e., those final states X with the same quantum numbers as the incident particle, contributes to $d\sigma/dt\,dM^2$, since the Pomeron carries the quantum numbers of the vacuum

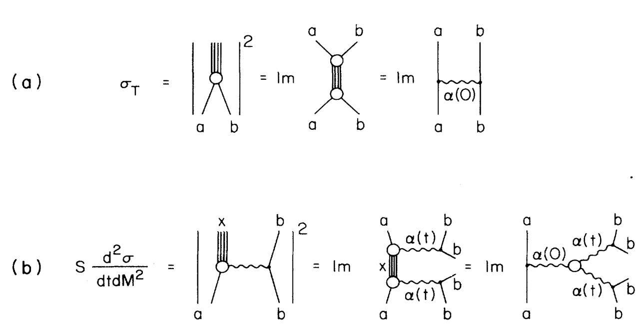

FIG. 5. Pomeron exchange diagrams for the total cross section and for single diffraction dissociation (triple-Pomeron diagram).

and thus cannot change those of the incident particle [a in Fig. 5(b)] at the vertex. Furthermore, the $1/M^2$ dependence guarantees that as $s \to \infty$ the final result is independent of the specific form of the coherence condition, in particular, the cutoff parameter a in the M^2 integration ($M^2_{\rm max} = as$), since it only contributes with a constant term ($\sim \ln a$).

However, although the nondiffractive contributions to Eq. (50) (e.g., from the Reggeon-Reggeon-Pomeron and π-π-Pomeron vertex) vanish for $s \to \infty$, they contribute at finite s. The value of the cutoff a is relevant in calculations of the diffractive part directly from the measured $d\sigma/dt\, dM^2$, and can be estimated as $a \approx 1/(2R_N m) \approx 0.1$. As can be seen in Fig. 4.13 of Ref. [36], for $M^2/s < 0.1$ the diffractive (triple-Pomeron) part gives the largest contribution to $d\sigma/dt\, dM^2$.

Integration of (51) leads to

$$\left(\frac{d\sigma_{\rm diff}}{dt}\right)_{t=0} = g_{PPP}\frac{\beta_P(0)^3}{16\pi^2} s_0 \ln(s/{\rm const}) \tag{52}$$

Together with (49) and (13) this result implies the logarithmic rise

$$\omega_\sigma = g_{PPP}\frac{\beta_P(0)}{\pi} s_0 \ln(s/{\rm const}) \tag{53}$$

observed in Sec. II.

As we already noted, in extrapolating to energies above 300 GeV one must take into account the rise of the nucleon-nucleon cross section. Inclusion of higher-order Pomeron diagrams (see, e.g., [44–46]) modifies the behavior of σ by logarithms of s and is able to describe the observed growth of the total cross section. In this case we also expect ω_σ to be modified by logarithmic terms. Instead of discussing the details of such a rather involved calculation in the "critical" [since one assumes $\alpha_P(0) = 1$] Pomeron-Reggeon field theory, we discuss the "supercritical" Pomeron model [47], in which one assumes

$$\alpha_P(0) = 1 + \epsilon, \tag{54}$$

and which leads to a $\sigma \sim s^\epsilon$ dependence, as can be seen from (48). Experimentally $\epsilon \approx 0.08$ [46]. This model is consistent with unitarity and the Froissart bound since the inclusion of multi-Reggeon exchanges alters the energy dependence of σ at very high energies (e.g., they contribute about 10% at energies reached at SPS [47]). At intermediate energies, where multi-Reggeon exchanges are not important, we can calculate $d\sigma_{\rm diff}/dt$ from (50)

$$\left(\frac{d\sigma_{\rm diff}}{dt}\right)_{t=0} = g_{PPP}\frac{\beta_P(0)^3}{16\pi^2}\left(\frac{s}{s_0}\right)^{2\epsilon}\frac{s_0}{\epsilon} \times\left[\left(\frac{s_0}{M^2_{\rm min}}\right)^\epsilon - \left(\frac{s_0}{as}\right)^\epsilon\right]. \tag{55}$$

The total cross section is given by $\sigma = \beta_P(0)(s/s_0)^\epsilon$, and for ω_σ one obtains

$$\omega_\sigma = g_{PPP}\frac{\beta_P(0)}{\pi}\frac{s_0}{\epsilon}\left[\left(\frac{s_0}{M^2_{\rm min}}\right)^\epsilon - \left(\frac{s_0}{as}\right)^\epsilon\right], \tag{56}$$

which leads to an asymptotically constant ω_σ. Inclusion of contributions from higher order diagrams may alter this result.

In Fig. 1 we indicate two possible predictions for ω_σ that follow from our theoretical estimates. On one hand we show an $\omega_\sigma \sim \ln s$ extrapolation following from Eq. (22), which is consistent with the single critical Pomeron exchange estimate, but which is probably an overestimate of ω_σ. The dashed curve is a fit of the form suggested by supercritical Pomeron exchange:

$$\omega_\sigma = b - c/s^\epsilon. \tag{57}$$

The parameters, b=0.843, c=0.96, ϵ=0.086, are chosen to reproduce roughly the values obtained from Murthy [19] and the intermediate set from Dakhno [22], with ϵ taken from [47]. We have not included in our fit the points in Fig. 1 for $p_{\rm lab} > 340$ GeV, since they are not tested by experiment and are obtained without a consistent treatment of σ and $d\sigma/dt\, dM^2$.

The extrapolations of ω_σ, although crude estimates, indicate that cross-section fluctuations become increasingly important in the RHIC energy range with a possible $\omega_\sigma \approx 0.4 - 0.5$. On the other hand, the UA4 data point suggests that the theoretical picture presented so far could change quite drastically between 1 TeV $\lesssim p_{\rm lab} \lesssim 100$ TeV (i.e., 40 GeV $\lesssim \sqrt{s} \lesssim$ 430 GeV). Sources of such a change are presently not very well understood. Increasing importance of Reggeon-Reggeon interactions could give rise to such behavior. However, according to Ref. [47], such corrections do not affect the total cross section by more than 10% at energies reached at SPS; their effect on the diffractive cross section could be larger. In a parton picture such a transition could arise from a strong impact parameter dependence of ω_σ, which would result from the shadowing of the interaction between partons. If, for example, the center of the nucleon becomes increasingly absorptive ("black") for all cross-section eigenstates, ω_σ would decrease and vanish in the limit of total absorption. We must await further experiment in order to clarify the picture.

VI. CONCLUSIONS

Cross-section fluctuations are not only important in the physics of heavy-ion collisions, but they present an interesting challenge to our understanding of the hadronic structure and the strong interaction at high energies as well. We have demonstrated how hadronic cross-section fluctuations can be consistently related to the physics of inelastic shadowing and diffractive dissociation. The dispersion of cross sections is determined by the mass distribution for diffractive scattering $d\sigma/dt\, dM^2$ at zero momentum transfer, and the total cross section. Experimental data show a broadening of the distribution $\sim \ln s$ up to at least $p_{\rm lab} = 1$ TeV. At higher energies there is a paucity of experimental information. Only one data point by the UA4 collaboration at $p_{\rm lab} \approx 160$ TeV suggests a change from rising fluctuations to a decrease with energy. Confirmation of this result is an interesting challenge for our understanding of hadronic interactions at high energies. While theoretical studies based on the triple-Pomeron limit can explain the initial rise of the fluctuations, extrapolations to higher energies remain ambiguous, due, e.g., to uncertainties in the theoretical sources of the energy dependence of σ_{NN}.

We have shown how the third moment of the cross-section distribution is probed in proton-deuteron diffractive dissociation. Using information on this moment together with the asymptotic behavior $P(\sigma \to 0) \sim \sigma$, which follows from quark counting rules, we have estimated the form of $P(\sigma)$. The value for $\langle\sigma^3\rangle$ derived from experiment suggests that $P(\sigma)$ falls off much more strongly than a Gaussian for $\sigma \gtrsim 1.7\bar{\sigma}$. Future determinations of $\langle\sigma^3\rangle$, via, e.g., diffraction or shadowing in light nuclei, could be very helpful in extracting information about $P(\sigma)$ and the parton structure of hadrons.

The fluctuations for a pionic projectile turn out to be almost a factor of 2 larger than for a nucleon. This result is understandable in a constituent quark picture due to the smaller number of valence degrees of freedom in the meson. Probing of these large fluctuations in π-nucleus (as well as K-nucleus) multiplicity and transverse energy distributions would be an interesting test for the idea of color opacity. Our findings imply that color transparency effects should be larger for meson-induced reactions, not only because of observed larger fluctuations in the π-N cross section, but also from quark counting rules which suggest that $P_{\rm meson}(\sigma \to 0) \sim$ const, whereas $P_N(\sigma)$ vanishes in this limt.

We predict that heavy-ion collisions will show a significant increase of fluctuations in multiplicities and transverse energy from CERN to RHIC energies [16, 28] if the physics of the triple-Pomeron limit is dominant at RHIC energies. These fluctuations are due to the initial state of the collision and should increase with energy as long as an independent multiple-scattering picture is valid. Therefore, knowledge of the energies at which these fluctuations disappear in various systems could serve as a useful signal about thermalization or a transition to new degrees of freedom.

ACKNOWLEDGMENTS

We thank B. Z. Kopeliovich for helpful discussions. This work was supported by NSF Grant No. PHY89-21025 and in part by DOE Grant No. DE-FG02-93 ER40771. B.B. is grateful for support from the Alexander von Humboldt Stiftung and H.H. for support from the Danish Natural Science Research Council.

[1] V.N. Gribov, Zh. Eksp. Teor. Fiz. **56**, 892 (1969) [Sov. Phys. JETP **29**, 483 (1969)].
[2] G. Bertsch, S.J. Brodsky, A.S. Goldhaber, and J.G. Gunion, Phys. Rev. Lett. **47**, 297 (1981).
[3] E.L. Feinberg and I.Y. Pomeranchuk, Suppl. Nuovo Cimento **III**, 652 (1956).
[4] M.L. Good and W.D. Walker, Phys. Rev. **120**, 1857 (1960).
[5] L.L. Frankfurt and M. Strikman, Nucl. Phys. **B250**, 143 (1985).
[6] S.J. Brodsky and P. Hoyer, Phys. Rev. Lett. **63**, 1566 (1989).
[7] F. Low, Phys. Rev. D **12**, 163 (1975).
[8] S. Nussinov, Phys. Rev. Lett. **34**, 1286 (1975).
[9] A.H. Mueller, in *Proceedings of the 17th Rencontre de Moriond: Elementary Hadronic Processes and New Spectroscopy*, Les Arcs, France 1982, edited by J. Tran Thanh Van (Editions Frontières, Gif-sur-Yvette, 1982), p. 13.
[10] S.J. Brodsky, in *Multiparticle Dynamics 1982*, Proceedings of the International Symposium, Volendam, Netherlands, 1982, edited by W. Kittel *et al.* (World Scientific, Singapore, 1983), p. 963.
[11] L.L. Frankfurt, Professor Habilitatus thesis, Leningrad (St. Petersburg), 1981.
[12] L.L. Frankfurt and M. Strikman, Phys. Rep. **76**, 215 (1981).
[13] L.L. Frankfurt and M. Strikman, Phys. Rev. Lett. **66**, 2289 (1991).
[14] L.L. Frankfurt and M. Strikman, Prog. Part. Nucl. Phys. **27**, 135 (1991).
[15] H. Heiselberg, G.A. Baym, B. Blättel, L.L. Frankfurt, and M. Strikman, Phys. Rev. Lett. **67**, 2946 (1991).
[16] B. Blättel, G. Baym, L.L. Frankfurt, H. Heiselberg, and M. Strikman, in *Quark Matter '91*, Proceedings of the Ninth International Conference on Ultrarelativistic Nucleus-Nucleus Collisions, Gatlinburg, Tennessee, edited by T. Awes *et al.* [Nucl. Phys. **A544**, 479c (1992)].
[17] R.J. Glauber, Phys. Rev. **100**, 242 (1955).
[18] V. Franco and R.J. Glauber, Phys. Rev. **142**, 1195 (1965).
[19] P.V.R. Murthy, C.A. Ayre, H.R. Gustafson, L.W. Jones, and M.J. Longo, Nucl. Phys. **B92**, 269 (1975).
[20] A.S. Carroll *et al.*, Phys. Lett. **61B**, 303 (1976).
[21] Note that we neglect in this derivation any correlation of fluctuations in the internal configurations of the bound proton and neutron in the deuteron. This approximation is correct in a description of the deuteron as two nucleons. Admixture of exotic components such as $\Delta\Delta$, six quark states, or pions, would lead to corrections. However, a significant admixture of exotics would effect the value of $\sigma_{\rm tot}(hd)$ at energies of a few GeV, where data agree well with the classical Glauber model. Current upper limits on these admixtures are rather tight, generally $< 1\%$ [see, e.g., L. L. Frankfurt and M. Strikman, Phys. Rep. **160**, 235 (1988), Chap. 2]; to a first approximation, these components can be neglected.
[22] L.G. Dakhno, Yad. Fiz. **37**, 993 (1983) [Sov. J. Nucl. Phys. **37**, 590 (1983)].
[23] A.B. Kaidalov and L.A. Kondratyuk, Nucl. Phys. **B56**, 90 (1973).
[24] D.R. Roy and R.G. Roberts, Nucl. Phys. **B77**, 240 (1974).
[25] R.D. Field and G.C. Fox, Nucl. Phys. **B80**, 367 (1974).
[26] Yu. M. Kazarinov *et al.*, Zh. Eksp. Teor. Fiz. **70**, 1152 (1976) [Sov. Phys. JETP **43**, 598 (1976)].
[27] B. Blättel, G. Baym, L.L. Frankfurt, and M. Strikman, Phys. Rev. Lett. **70**, 896 (1993).
[28] G. Baym, B. Blättel, L.L. Frankfurt, H. Heiselberg, and M. Strikman (unpublished).
[29] H. Miettinen and J. Pumplin, Phys. Rev. D **18**, 1696 (1978); Phys. Rev. Lett. **42**, 204 (1979).
[30] J. Pumplin, Phys. Scripta **25**, 191 (1982).

[31] M.G. Albrow *et al.*, Nucl. Phys. **B108**, 1 (1976).
[32] D. Bernard *et al.*, Phys. Lett. B **186**, 227 (1987).
[33] From very recently reported data from the Fermilab Tevatron at $\sqrt{s} = 1800$ GeV [J. Orear, talk at the workshop on small-x and diffractive physics at the Fermilab Tevatron, 1992] one can infer a value of $\omega_\sigma \approx 0.17$. However the value of ω_σ inferred from the collider data is really a lower bound since diffractive dissociation into low mass excitations has not been measured, and may significantly increase ω_σ at collider energies. We are indebted to K. Goulianos for an explanation of this point.
[34] B. Z. Kopeliovich and L. I. Lapidus, Pis'ma Zh. Eksp. Teor. Fiz. **28**, 664 (1978) [JETP Lett. **28**, 614 (1978)].
[35] Y. Akimov *et al.*, Phys. Rev. D **14**, 3148 (1976).
[36] J. Alberi and G. Goggi, Phys. Rep. **74**, 1 (1981).
[37] A.B. Zamolodchikov, B.Z. Kopeliovich, L.I. Lapidus, and S.V. Mukhin, Zh. Eksp. Teor. Fiz. **77**, 451 (1979) [Sov. Phys. JETP **50**, 229 (1979)].
[38] K.S. Kölbig and B. Margolis, Nucl. Phys. **B6**, 85 (1968).
[39] D.F. Nitz, Ph.D. thesis, University of Rochester, 1977.
[40] Y. Akimov *et al.*, Phys. Rev. Lett. **39**, 1432 (1977); **40**, 1159(E) (1978).
[41] T. Regge, Nuovo Cimento **14**, 951 (1959); **18**, 947 (1960); G.F. Chew and S. Frautschi, Phys. Rev. **123**, 1478 (1961); V.N. Gribov, Zh. Eksp. Teor. Fiz. **41**, 667 (1961) [Sov. Phys. JETP **14**, 478 (1962)]; G.F. Chew, S. Frautschi, and S. Mandelstam, Phys. Rev. **126**, 1202 (1962).
[42] For an introduction see, e.g., H. Muirhead, *The Physics of Elementary Particles* (Oxford, England, 1965); P.D.B. Collins, *An Introduction to Regge-Theory and High Energy Physics* (Cambridge University Press, Cambridge, England, 1977).
[43] K. Goulianos, Phys. Rep. **101**, 169 (1983).
[44] A.A. Migdal, A.M. Polyakov, and K.A. Ter Martirosyan, Pis'ma Zh. Eksp. Teor. Fiz. **19**, 239 (1974) [JETP Lett. **19**, 147 (1974)].
[45] A. White, in *Proton-Antiproton Collider Physics*—1981, Proceedings of a Workshop Sponsored by the University of Wisconsin, the Department of Energy, and the National Science Foundation, edited by V. Barger, D. Cline, F. Halzen, AIP Conf. Proc. No. 85 (American Institute of Physics, New York, 1982), p. 362.
[46] M.M. Block and A. White, in *Proceedings of the 21st International Symposium on Multiparticle Dynamics*, Wuhan, China, 1991, edited by L. Liu and Y. Wu (World Scientific, Singapore, 1992).
[47] A. Donnachie and P.V. Landshoff, Nucl. Phys. **B267**, 690 (1986); Part. World **2**, 7 (1991).